Supporting Information (SI)

Delamination-Free In-Air and Underwater Oil-Repellent Filters for Oil-Water Separation: Gravity-Driven and Cross-Flow Operations

Bishwash Shrestha[†], *Mohammadamin Ezazi*[†], *Gibum Kwon* *

Department of Mechanical Engineering, University of Kansas, Lawrence, Kansas 66045, United States.

*Email: gbkwon@ku.edu

[†] indicating equal contributions

Section S1. Fourier-transform infrared (FT-IR) spectroscopy analysis of F-PEGDA.

To verify the chemical structure of F-PEGDA, the FT-IR analysis was conducted using a Perkin Elmer Spectrum 400 Spectrometer. The FT-IR spectra were recorded at a resolution of 4 cm^{-1} for 16 scans. **Fig. S1** demonstrates the survey spectra of F-PEGDA prepared with varied compositions of F-acrylate. Peaks appearing at ≈ 1205 cm^{-1} and 1149 cm^{-1} (pink shade) confirm the presence of fluorine moieties ($-CF_2$) [1]. The fluorine moieties are critical for lowering the overall solid surface free energy. Note that these peaks become more prominent as the F-acrylate concentration increases in the F-PEGDA. Peaks corresponding to hydroxyl group (-OH, 948 cm^{-1}, blue shade) and carbonyl group (-CO, 1440-1395 $cm^{-1}$and 1720 cm^{-1}, green shades) are also shown in FT-IR spectra [2, 3].

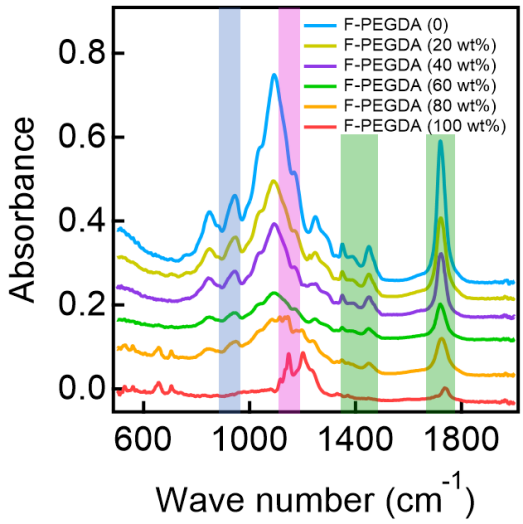

Figure S1. FT-IR survey spectra of F-PEGDA prepared with varied compositions of F-acrylate.

Section S2. Effect of F-PEGDA solution viscosity on the pore size of a filter.

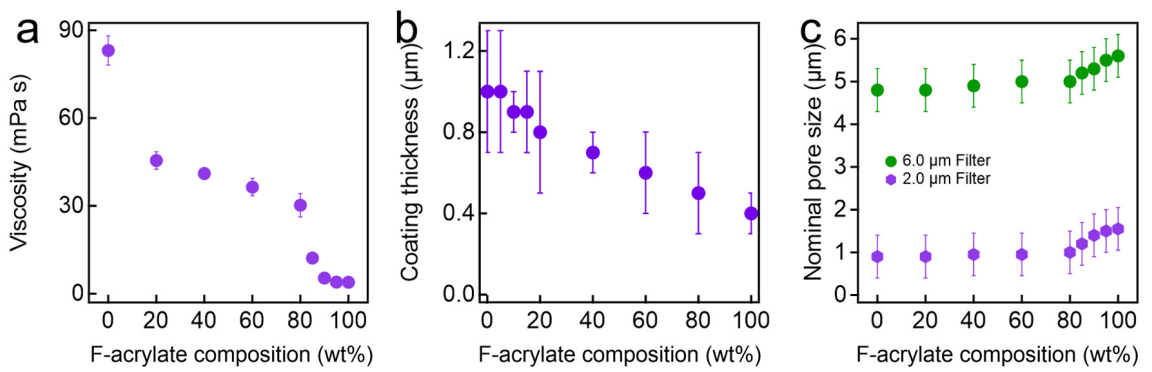

Figure S2. (a) The measured viscosity values of F-PEGDA solutions as a function of F-acrylate compositions. (b) The thickness of F-PEGDA coating as a function of F-acrylate compositions. (c) The nominal pore size of the resulting filters after F-PEGDA coating.

Fig. S2a demonstrates a plot of the viscosity as a function of F-acrylate composition in the F-PEGDA solution. The viscosity of the solution increases with a decrease in the F-acrylate

composition. We attribute this to a higher viscosity value of PEGDA in comparison to F-acrylate. We also found that an F-PEGDA coating solution with higher viscosity results in a coating with a higher thickness (**Fig. S2**b). As a consequence, the effective pore size of a filter is also affected by the coating solution viscosity. **Fig. S2**c shows that as F-acrylate composition decreases in the F-PEGDA coating solution, the nominal pore size of the resulting filter decreases as well. Based on these measurements, we anticipate that our F-PEGDA coating can be applied to a filter with a pore size of ≈1 μm or greater without resulting in a complete pore-clogging.

Section S3. Initial contact angles and Time of Wetting values for water on F-PEGDA surfaces.

When our F-PEGDA surface is subjected to water, it reconfigures by enabling the hydrophilic moieties (e.g., -OH groups) to emerge on the surface. This is a kinetic process that is manifested by the so-called Time of Wetting (ToW, see also main text). On our F-PEGDA surfaces, a sessile water droplet exhibits a finite initial contact angle upon being placed. Then, it gradually wets the surface. **Table S1** lists the measured initial contact angle values for water on F-PEGDA surfaces. **Fig. S3** shows the measured ToW values. It should be noted that a water droplet shows a final contact angle of 25°± 3° on the F-PEGDA (80 wt%) surface (also see **Fig. 1**c in main text). We determined the final contact angle when it remains unchanged (< 2°) for 10 mins.

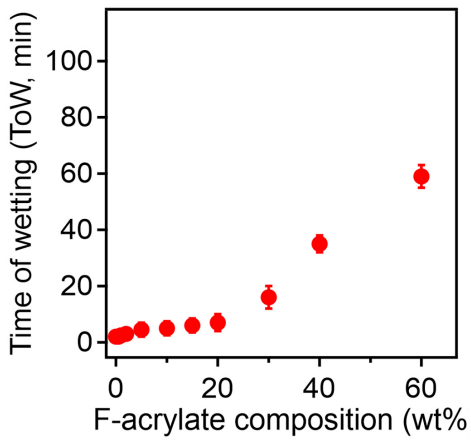

Figure S3. The measured ToW values for a sessile water droplet on the F-PEGDA surfaces with varying F-Acrylate compositions.

Table S1. The measured initial contact angles for a sessile water droplet (5 μl) on F-PEGDA surfaces with varying F-Acrylate compositions.

Surface	$\theta^*_{water,adv}$ (t=0)	$\theta^*_{water,rec}$(t=0)
F-PEGDA (0)	43°± 3°	0°
F-PEGDA (5 wt%)	62°± 2°	0°
F-PEGDA (10 wt%)	75°± 3°	0°

F-PEGDA (15 wt%)	82°± 2°	0°
F-PEGDA (20 wt%)	89°± 4°	0°
F-PEGDA (40 wt%)	95°± 5°	15°± 4°
F-PEGDA (60 wt%)	102°± 2°	25°± 3°
F-PEGDA (80 wt%)	110°± 3°	49°± 4°

Section S4. Calculation of the solid surface energy of F-PEGDA surfaces.

We have utilized the Owens and Wendt approach [4] to calculate the solid surface energy (γ_{sv}) of F-PEGDA surfaces with varying F-acrylate compositions. Note that we fabricated a smooth surface of F-PEGDA by spincasting. Two probe liquids, n-hexadecane (γ_{lv} =27.5 mN/m) and water (γ_{lv}^{d}=21.1 mN/m and γ_{lv}^{p}=51.0 mN/m) were used as a non-polar liquid and a polar liquid, respectively. **Table S2** lists the calculated solids surface energy values of F-PEGDA surfaces with varying F-acrylate compositions.

Table S2. The calculated solid surface energy values of F-PEGDA surfaces.

Surface	γ_{sv}^{p} (mN m^{-1})	γ_{sv}^{d} (mN m^{-1})	γ_{sv} (mN m^{-1})
F-PEGDA (0)	39.5	35.2	74.7
F-PEGDA (5 wt%)	24.6	15.3	39.9
F-PEGDA (10 wt%)	13.8	13.2	27.0
F-PEGDA (15 wt%)	6.2	11.2	17.4
F-PEGDA (20 wt%)	3.1	10.1	13.2
F-PEGDA (40 wt%)	0.9	9.9	10.8
F-PEGDA (60 wt%)	0.5	9.9	10.4
F-PEGDA (80 wt%)	0.5	9.9	10.4

Section S5. Apparent contact angles for water and oil on F-PEGDA coated filter with 2.0 µm of inherent pore size.

Fig. S4 demonstrates plots of advancing and receding apparent contact angles of DI water and oil (n-hexadecane) on a filter with 2.0 µm of inherent pore size that was coated with F-PEGDA with varied F-acrylate compositions. Similar to the results for the 6.0 µm filter (see **Fig. 1**c in main text), the apparent contact angles of oil increase with an increase in the composition of F-acrylate. At 20 wt.% of F-acrylate composition, the advancing ($\theta^*_{oil,\ adv}$) and receding ($\theta^*_{oil,\ rec}$) apparent contact angles for oil were measured as 135°± 3° and 111°±3°, respectively, while those for water remained zero ($\theta^*_{water,\ adv}$ = 0° and $\theta^*_{water,\ rec}$ = 0°). When the F-acrylate composition becomes 80 wt.% in F-PEGDA coating, the value of $\theta^*_{water,\ adv}$ is measured as 18°± 3°.

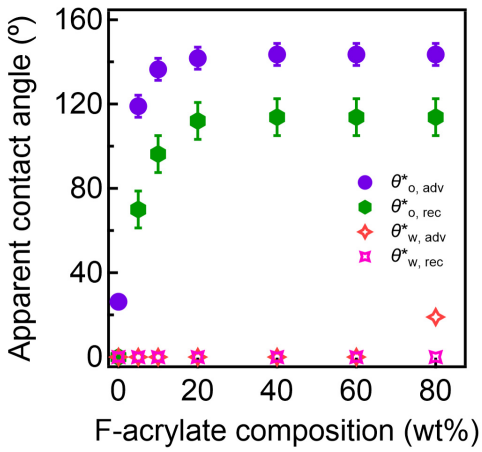

Figure S4. Advancing and receding apparent contact angles for water and oil (n-hexadecane) on F-PEGDA surface with varied compositions of F-acrylate for the filter with 2.0 µm of inherent nominal pore size.

Section S6. Apparent contact angles for oil on a filter submerged in water.

Fig. S5 demonstrates a plot of advancing and receding apparent contact angles for oil (n-hexadecane) on filters coated with F-PEGDA with various F-acrylate compositions submerged in DI water. The results show that the filters coated with F-PEGDA exhibited very high underwater apparent oil contact angles (i.e., underwater superoleophobic wettability). Further, a filter coated with F-PEGDA with a lower F-acrylate composition exhibits a higher underwater oil contact angle. For example, a filter coated with F-PEGDA (20 wt.%) exhibited contact angles of $\theta^*_{oil,\ adv\ (under\ water)}$ = 169°± 2° and $\theta^*_{oil,\ rec}$

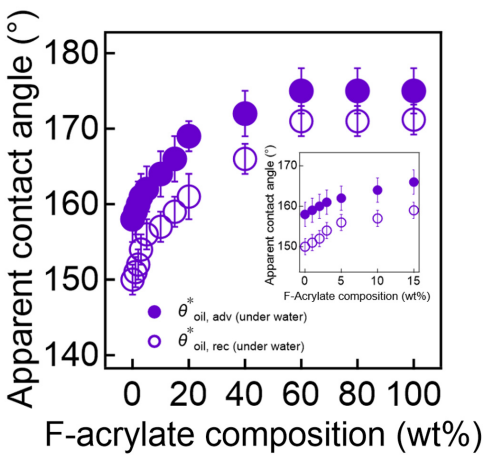

Figure S5. Underwater advancing and receding apparent contact angles of oil (n-hexadecane) on F-PEGDA coatings prepared with varied F-acrylate compositions.

$_{(under\ water)}$ = 161°± 3°, whereas the one coated with F-PEGDA (80 wt.%) exhibited $\theta^*_{oil,\ adv\ (under\ water)}$ = 174°± 3° and $\theta^*_{oil,\ rec\ (under\ water)}$ = 171°±2°.

Section S7. Measurements of water uptake by F-PEGDA coated filters.

The measurement of the water uptake by F-PEGDA coated filters is conducted by submerging the filter (2.5 cm × 2.5 cm) into a water bath (250 mL) for 1 hour. We measured the weight of the filter after 1 hour and compared it with that of the dry (i.e., as-prepared) one. **Table S3** lists the measured weights of filters. The water uptake is calculated by subtracting the weight of an as-prepared filter from that of the wet filter.

Table S3. The measured weight values of F-PEGDA (20 wt%) coated filters and calculated water uptake.

Filter	Dry filter (mg)	Wet filter (mg)	Water uptake (mg)
6.0 µm	160	365	205
2.0 µm	162	381	219

Section S8. Delamination of F-PEGDA coating from a filter without MEMO grafting.

Grafting MEMO to a filter surface can prevent the delamination of F-PEGDA coating. **Fig. S6**a and **S6**b show SEM images with the EDS data (e.g., elemental mapping) of a filter coated with F-PEGDA (20 wt.%) without MEMO grafting before and after submersion in water for 1 hour, respectively. The results show that the Fluorine (F) element nearly disappeared after 1 hour of submersion, indicating that the F-PEGDA coating is delaminated (see **Fig. S6**b).

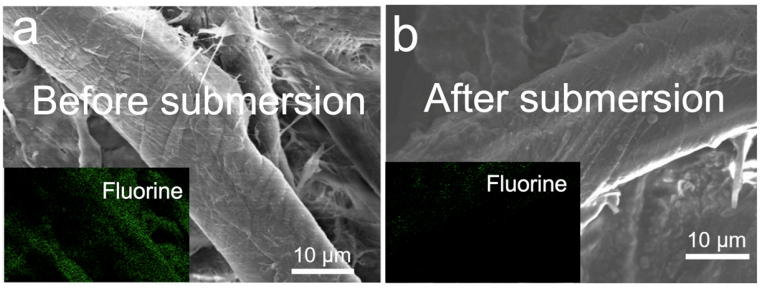

Figure S6. (a-b) SEM images and the EDS data (elemental mapping) showing a filter surface coated with F-PEGDA without MEMO before (a) and after submersion in water for 1 hour (b).

Section S9. Size distribution of the dispersed phases in oil-water emulsions.

Dynamic light scattering (DLS) was utilized to determine the size distribution of the dispersed phases in oil-water emulsions. **Fig. S7**a and **S7**b show that the average size of the oil droplets dispersed in water is ≈19 μm, whereas the average size of the water droplets dispersed in the oil phase is ≈16 μm.

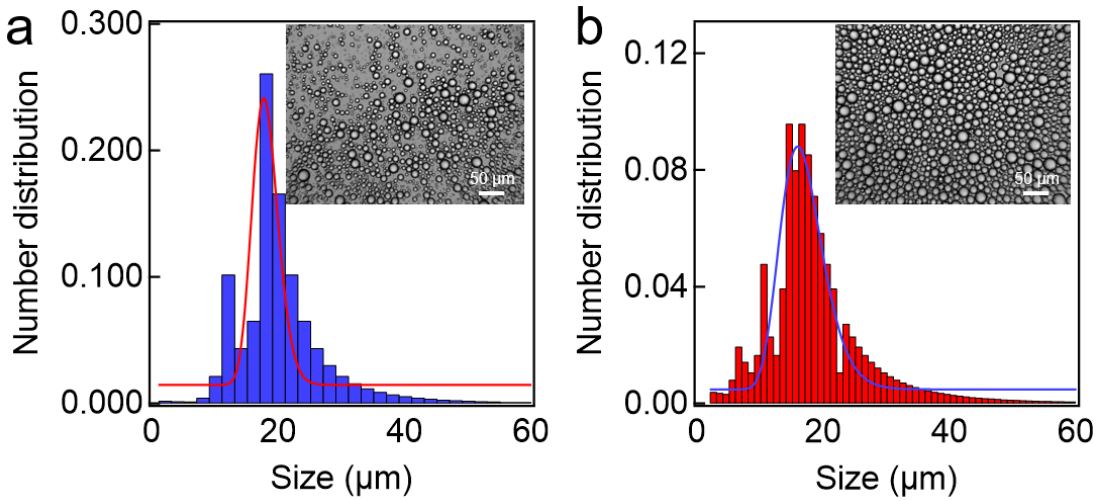

Figure S7. Size distribution of dispersed oil droplets in (a) SDS-stabilized oil-in-water emulsion and (b) dispersed water droplets in Tween 80-stabilized water-in-oil emulsion. The insets show the optical microscopy images of dispersed phases.

Section S10. TGA data for permeates from continuous separation of oil-water emulsion by cross-flow apparatus.

We determined the separation efficiency by using PerkinElmer PYRIS 1 thermogravimetric analysis (TGA). About 50 mg of a sample was heated from room temperature to 105 °C at a rate of 5 °C min^{-1}. The temperature was held constant at 105 °C for 60 minutes. **Fig. S8** shows the TGA plots of the water-rich permeates through the filters with 2.0 μm and 6.0 μm of inherent nominal pore size coated with F-PEGDA (20 wt.%) after continuous separation of oil-in-water emulsion using a cross-flow cell. It is observed that a 2.0 μm pore size filter was able to separate oil and water

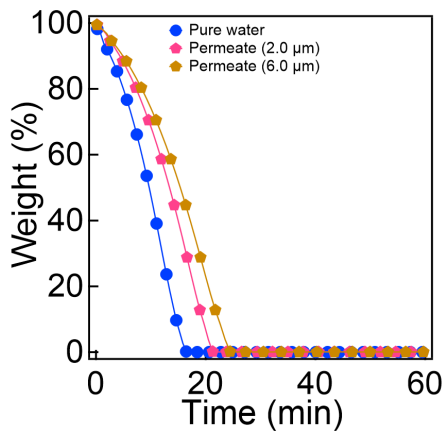

Figure S8. TGA analysis of the permeates and pure water for cross-flow apparatus-based separation.

at the high efficiency of ≈98%, while the one with a 6.0 μm of pore size demonstrated a separation efficiency of ≈96%.

Section S11. The measured flux values of continuous separation of oil-in-water emulsion.

Fig. S9 shows the measured flux values for the water-rich permeates during the continuous separation of oil-in-water emulsion utilizing F-PEGDA (20wt%) coated filters. The results show that the flux values were maintained at 204 ± 4 L m^{-2} h^{-1} (6.0 μm filter) and 172 ± 5 L m^{-2} h^{-1} (2.0 μm filter) over 50 hours of continuous separation.

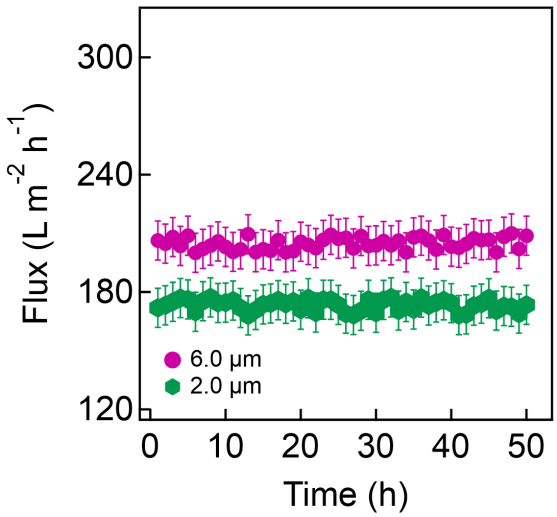

Figure S9. Measured flux values for the water-rich permeates as a function of time.

References

1. Kumar, V.; Pulpytel, J.; Mannelli, I.; Rossi, F.; Rauscher, H.; Arefi-Khonsari, F. In *Low surface energy fluorocarbon coatings via plasma polymerization process: process optimization and protein repellent study*, International Symposium on Plasma Chemistry, 2009; 2009.
2. Browning, M.; Cereceres, S.; Luong, P.; Cosgriff-Hernandez, E., Determination of the in vivo degradation mechanism of PEGDA hydrogels. *Journal of Biomedical Materials Research Part A* **2014,** 102, (12), 4244-4251.
3. Zhang, X.; Yang, D.; Nie, J., Chitosan/polyethylene glycol diacrylate films as potential wound dressing material. *International journal of biological macromolecules* **2008,** 43, (5), 456-462.
4. Owens, D. K.; Wendt, R., Estimation of the surface free energy of polymers. *Journal of applied polymer science* **1969,** 13, (8), 1741-1747.